PHYSICAL REVIEW B **90**, 220504(R) (2014)

Superconductor derived from a topological insulator heterostructure

Satoshi Sasaki, Kouji Segawa, and Yoichi Ando*
Institute of Scientific and Industrial Research, Osaka University, Ibaraki, Osaka 567-0047, Japan
(Received 7 April 2014; revised manuscript received 19 November 2014; published 1 December 2014)

Topological superconductors (TSCs) are of significant current interest because they offer promising platforms for finding Majorana fermions. Here we report on a superconductor synthesized by intercalating Cu into a naturally formed topological insulator (TI) heterostructure consisting of Bi_2Se_3 TI units separated by nontopological PbSe units. Interestingly, in this TI-based superconductor, the specific-heat behavior suggests the occurrence of unconventional superconductivity with gap nodes. The existence of gap nodes in a strongly spin-orbit coupled superconductor would give rise to spin-split Andreev bound states that are the hallmark of topological superconductivity. Hence, this superconductor emerges as an intriguing candidate TSC.

DOI: 10.1103/PhysRevB.90.220504 PACS number(s): 74.10.+v, 74.25.Bt, 74.70.Dd, 74.78.Fk

A major theme in current condensed matter physics is to understand and explore the roles of topology in quantum mechanics. In topological insulators (TIs), a nontrivial topology of the quantum-mechanical wave functions leads to the appearance of gapless conducting states at the boundary (i.e., edge or surface) [1–3]. Topological superconductors (TSCs) are conceptually similar to TIs and are characterized by gapless quasiparticle states at the boundary [1,4–6], but an important distinction from TIs is that the boundary state of a TSC is a good place to look for Majorana fermions [7–9], which possess a distinct property that particles are their own antiparticles and would be useful for fault-tolerant topological quantum computing. In this context, superconductors derived from TIs are of particular interest, because the strong spin-orbit coupling inherent to TIs may lead to unconventional pairing that is a prerequisite to TSCs [9]. However, there have been only a few cases in which superconductivity is found in doped TIs [10–16], and it is strongly desired that a superconductor with promising indications of unconventional superconductivity be discovered in a doped TI.

Recently, two of the authors have contributed to the discovery of an interesting topological insulator [17], $(PbSe)_5(Bi_2Se_3)_6$. This is a member of the Pb-based homologous series of compounds [18], $(PbSe)_5(Bi_2Se_3)_{3m}$ ($m = 1,2,\ldots$), which form natural multilayer heterostructures of a topological insulator (Bi_2Se_3) and an ordinary insulator (PbSe). It was found that at $m = 2$, the PbSe unit works as a block layer and the topological boundary states are encapsulated in each Bi_2Se_3 unit, making the system to possess quasi-two-dimensional (quasi-2D) states of topological origin throughout the bulk [17]. Hence, the $m = 2$ material is a peculiar type of TI filled with quasi-2D topological bands that originate due to the nontrivial Z_2 topology of the Bi_2Se_3 unit. Bi_2Se_3 consists of a stack of Se-Bi-Se-Bi-Se quintuple layers (QLs), and the $m = 2$ member of $(PbSe)_5(Bi_2Se_3)_{3m}$ has 2 QLs in its Bi_2Se_3 unit [see Fig. 1(a)]. In the middle of this 2-QL unit is a van der Waals gap, into which intercalations of atoms or molecules are possible.

Motivated by the occurrence of superconductivity in Bi_2Se_3 upon Cu intercalation [10,19], we tried to make $(PbSe)_5(Bi_2Se_3)_6$ (hereafter called PSBS) superconducting via Cu intercalation. We first grew high-quality, single-phase crystals of PSBS ($m = 2$) with an improved method [20], and adopted the electrochemical technique which we developed for making high-quality $Cu_xBi_2Se_3$ superconductors [19]; as a result, we have succeeded in synthesizing a superconductor [20]. Intriguingly, this material, $Cu_x(PbSe)_5(Bi_2Se_3)_6$ (called CPSBS), turned out to be quite different from its cousin, $Cu_xBi_2Se_3$: First, this superconductor presents an unusual specific-heat behavior which suggests unconventional superconductivity. Second, nearly 100% superconducting samples can sometimes be synthesized, which makes it easier to elucidate its intrinsic nature.

Figure 1(b) shows the resistivity data for PSBS and CPSBS ($x = 1.36$). The Cu intercalation causes a sharp superconducting transition at 2.85 K, and at the same time, it introduces moderate electron scattering to enhance the residual resistivity. The carrier density increases from $n_e \simeq 4 \times 10^{20}$ in PSBS to 1.2×10^{21} cm^{-3} in CPSBS ($x = 1.36$), which suggests that each intercalated Cu introduces about 0.7 electrons on average [20]. The Hall resistivity data indicate that the transport is governed by only one band (see Fig. S1(b) of the Supplemental Material [20]), suggesting that the topological and nontopological bands of the Bi_2Se_3 unit [17] may well have merged at the chemical potential of CPSBS. Such a merger does not preclude the occurrence of bulk topological superconductivity [21].

As shown in Figs. 1(c) and 1(d), in the present set of samples the onset of superconductivity was essentially independent of x and was always around 2.9 K for $x = 0.3$–2.3, whereas the shielding fraction (the fraction of the sample volume from which the magnetic field is kept out due to superconductivity after zero-field cooling) was very much sample dependent; note that, in the case of type-II superconductors, the shielding fraction is a better measure of the superconducting volume fraction than the Meissner fraction measured upon field cooling, because the latter is significantly affected by flux trapping. The random nature of the obtained shielding fraction vs x signifies the difficulty in synthesizing a homogeneous superconductor with intercalation, and apparently the Cu atoms in the majority of our samples are inhomogeneously

*y_ando@sanken.osaka-u.ac.jp

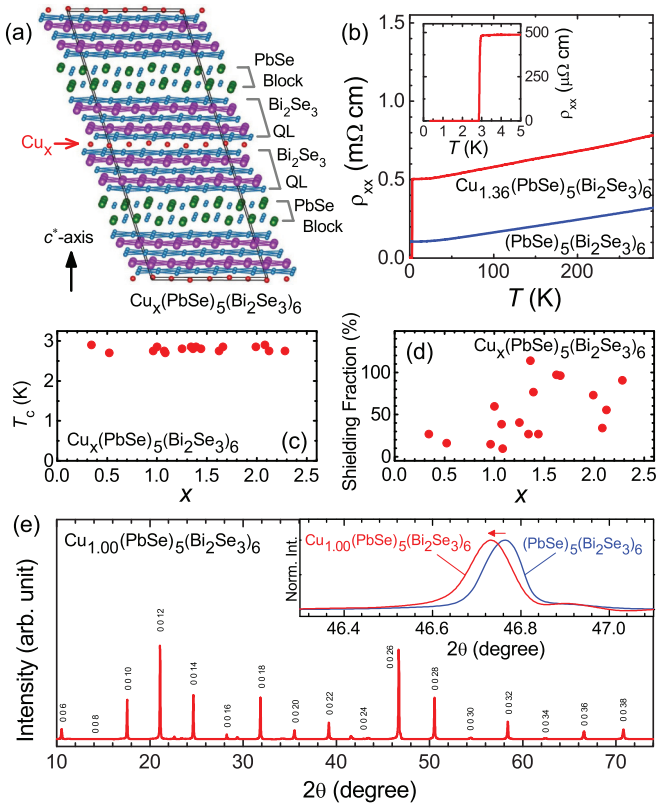

FIG. 1. (Color online) $Cu_x(PbSe)_5(Bi_2Se_3)_6$ superconductor. (a) Crystal structure [32] based on the data for PSBS [18]. Cu atoms are intercalated into the van der Waals gaps marked by red arrow. (b) Temperature dependencies of the resistivity ρ_{xx} for PSBS and CPSBS ($x = 1.36$). Inset shows the sharp superconducting transition at 2.85 K. (c) Onset T_c measured by dc magnetic susceptibility for samples with various x values. (d) Shielding fractions of the samples presented in (c) at 1.8 K. (e) XRD pattern measured on a cleaved surface (ab plane) of a superconducting CPSBS sample with $x = 1.00$ (shielding fraction ∼60%), where the peak pattern is essentially the same as that of pristine PSBS. Inset compares the positions of the prominent (0 0 26) peak for PSBS and CPSBS, which demonstrates that the periodicity perpendicular to the layers is slightly enlarged from 50.460(1) Å to 50.508(1) Å after the Cu intercalation.

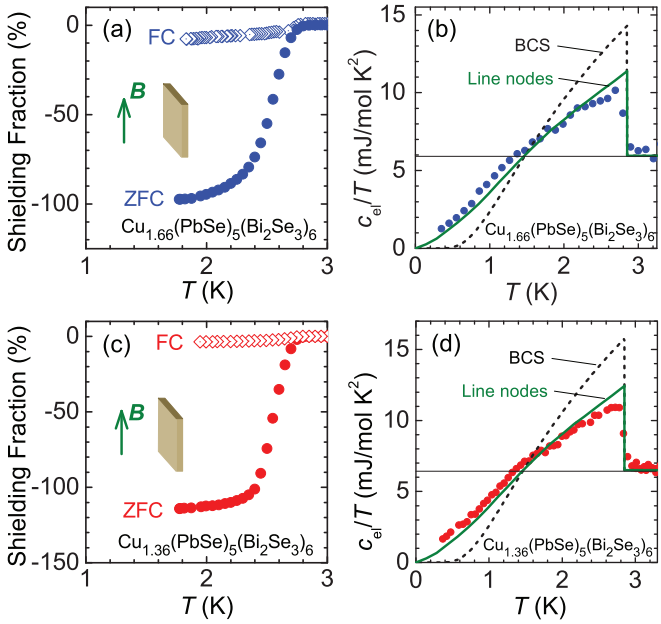

FIG. 2. (Color online) Shielding fraction and specific heat. (a) and (c) Temperature dependencies of the dc magnetic susceptibility measured in 0.2 mT applied parallel to the ab plane with the field-cooling (FC) and zero-field-cooling (ZFC) procedures for (a) $x = 1.66$ and (c) $x = 1.36$, presented in terms of the shielding fraction. Since the demagnetization effect is minimal for this geometry and the sample shape was irregular, we did not make any correction for it [the $x = 1.66$ (1.36) sample was 0.23 (0.16) mm thick and 1.6 ± 0.3 (1.7 ± 0.35) mm long along the B field]. (b) and (d) Superconducting transition in c_{el}/T in 0 T obtained after subtracting the phonon contribution determined in 2 T (see Fig. S2 [20]). The dashed line is the weak-coupling BCS behavior (coupling constant $\alpha = 1.76$) for T_c of 2.85 K. The green solid line is the theoretical curve for d-wave pairing on a simple cylindrical Fermi surface with line nodes along the axial direction [23]. Horizontal solid line corresponds to γ_N.

intercalated; nevertheless, we have confirmed that the superconducting portion is not forming a "shell" in our samples [20]. Furthermore, we have been able to achieve essentially 100% shielding fraction in a few samples with $x = 1.3$–1.7, and in those special samples the roles of the nonsuperconducting phase can be largely neglected. The x-ray diffraction (XRD) data from cleaved surfaces of single-crystalline CPSBS indicate that the system essentially preserves the same crystal structure of PSBS with a slightly elongated c^* axis, as is expected for an intercalated material [Fig. 1(e)]; however, it is beyond the scope of this Rapid Communication to precisely determine the crystallographic structure, including the exact position of Cu, of this complicated material with a large unit cell.

In the following, we focus on two samples with $x = 1.36$ and 1.66, which presented essentially 100% shielding fractions as shown in Figs. 2(a) and 2(c). Figures 2(b) and 2(d) show the behavior of the electronic specific heat c_{el} in terms of c_{el}/T vs T for the two samples; those data were obtained after subtracting the phonon contribution determined in 2 T described in Fig. S2 of the Supplemental Material [20]. The two samples consistently present two unconventional features that become apparent when compared with the conventional weak-coupling BCS behavior [22] shown with dashed lines: First, the jump height at T_c is much smaller than the prediction of the BCS theory, $1.43\gamma_N$, where γ_N is the normal-state electronic specific-heat coefficient corresponding to the horizontal solid lines. Second, c_{el}/T decreases much more slowly than the BCS behavior; in particular, c_{el}/T keeps showing a sizable temperature dependence even at our lowest temperature of 0.35 K ($T/T_c = 0.12$), whereas c_{el}/T should already become negligible at such a low temperature in the BCS case. (Strong-coupling BCS theory makes these discrepancies worse.) It is reassuring that those unconventional features are exactly reproduced in two different samples.

Such a peculiar behavior in c_{el}/T suggests the existence of nodes in the superconducting gap for the following reasons: First, when the gap has nodes, the averaged gap magnitude becomes smaller than the fully gapped case,

and the specific-heat jump is naturally reduced [6,22]; the green solid line in Figs. 2(b) and 2(d) gives an example for the d-wave superconductivity with line nodes [23]. Second, in contrast to the conventional BCS case in which $c_{\rm el}/T$ decreases exponentially at low T because of a finite activation energy, the existence of nodes allows thermal excitations of quasiparticles down to very low temperatures, changing the T dependence of $c_{\rm el}/T$ from exponential to a power law [6].

As one can see in Figs. 2(b) and 2(d), our data, particularly the strong T dependence near 0 K, bear striking similarity to the theoretical $c_{\rm el}/T$ behavior expected for a superconductor with line nodes [23], which points to the realization of unconventional superconductivity in CPSBS. Of course, specific-heat measurements alone are not sufficient for unambiguously nailing down the existence of nodes, because a multiband superconductor with a very small gap in one of the bands or an anisotropic s-wave superconductor with very small gap minima would give rise to a $c_{\rm el}/T$ behavior similar to what we found in CPSBS. Hence, phase-sensitive measurements are crucially important in the future research of this material. Also, STM and NMR experiments would be very useful for elucidating the unconventional superconductivity.

Note that in the case of nodal superconductors, impurity scattering causes a finite density of quasiparticle states at 0 K, causing $(c_{\rm el}/T)_{T\to 0}$ to be finite even in a 100% superconducting sample; this may also be the case in the present system, given the relatively large residual resistivity. Also, it is prudent to mention that the spin-orbit scattering [24] is pair breaking and may mimic the $c_{\rm el}/T$ behavior observed here, so its role should be elucidated in future. Nevertheless, it is fair to note that in $Cu_xBi_2Se_3$, where the spin-orbit scattering should be of similar strength, the $c_{\rm el}/T$ behavior was found to obey the BCS theory [19].

Due to the quasi-2D nature of the parent material PSBS [17], the superconductivity in CPSBS is likely to be realized on a quasi-2D Fermi surface, which is distinct from the three-dimensional (3D) bulk Fermi surface of Bi_2Se_3. This implies that the theory of 3D topological superconductivity proposed for $Cu_xBi_2Se_3$ [9] is not directly applicable. Nevertheless, it is still expected that strong spin-orbit coupling responsible for the topological nature of the parent material causes the effective pairing interaction to become spin dependent, which would lead to unconventional superconductivity [9]. When the Fermi surface is quasi-2D, a node in the unconventional superconducting gap is naturally extended along the c^* axis, forming a line node in the 3D Brillouin zone. It is thus expected that, if gap nodes were to be present in CPSBS, the $c_{\rm el}/T$ behavior should be close to that of a superconductor with line nodes.

The possible existence of line nodes in CPSBS is further supported by the magnetic-field dependence of the specific heat. Figure 3(a) shows the $c_{\rm el}/T$ vs T plots for various magnetic fields applied perpendicular to the ab plane described in Fig. S2 of the Supplemental Material [20], from which we extract the magnetic-field dependence of $c_{\rm el}$ at the lowest temperature, 0.35 K; here, to make our best effort to quantify its behavior, the data are corrected for a small Schottky anomaly [20], which is only $\lesssim 20\%$ even at the upper critical field and is comparable to the error bar. The obtained $c_{\rm el}(B)$ behavior at 0.35 K [Fig. 3(b)] is clearly nonlinear in B. Note that in conventional BCS superconductors $c_{\rm el}$ increases essentially linearly with B, because the number of induced quasiparticles is proportional to the number of vortices. On the other hand, in nodal superconductors, the Doppler shift of the quasiparticle excitations (so-called Volovik effect) causes more quasiparticles to be created per vortex than in the BCS case [25]; for line nodes, Volovik showed [25] that $c_{\rm el}$ increases as $\sim\sqrt{B}$. Indeed, our data are best described with $c_{\rm el} \sim B^{0.5}$, supporting the existence of line nodes.

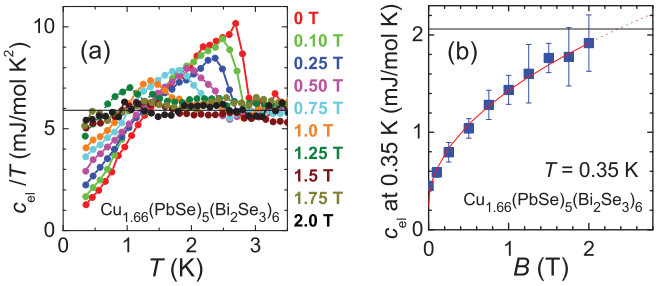

FIG. 3. (Color online) Specific heat in magnetic fields. (a) Temperature dependencies of $c_{\rm el}/T$ in various magnetic fields ($B \perp ab$) for $x = 1.66$. Small Schottky anomaly that becomes nonnegligible above $\sim$1.5 T has been subtracted (see [20]). Horizontal solid line corresponds to $\gamma_{\rm N}$. (b) Magnetic-field dependence of $c_{\rm el}$ at 0.35 K taken from the data in (a). The red solid line is the best fit of the function $aB^n + c_0$ to the data, yielding $n = 0.50 \pm 0.06$, $a = 1.2 \pm 0.1$ (mJ mol^{-1} K^{-1} T^{-n}), and $c_0 = 0.25 \pm 0.09$ (mJ mol^{-1} K^{-1}). Horizontal solid line corresponds to $\gamma_{\rm N}T$ at $T = 0.35$ K.

Figures 4(a) and 4(c) show the magnetic-field-induced resistive transitions at various temperatures in $B \perp ab$ and in $B \| ab$, respectively, from which the resistive upper critical fields $B_{c2\perp}(T)$ and $B_{c2\|}(T)$ are extracted. We plot in Figs. 4(b) and 4(d) the magnetic field values at which 2%, 50%, and 98% of the normal-state resistivity $\rho_{\rm N}$ is recovered at a given temperature. It is customary to use 50% $\rho_{\rm N}$ for defining B_{c2} [13,14,26]. In Fig. 4(b), the onset temperatures of the specific-heat transitions in $B \perp ab$ determined for the same sample (see Fig. S5(a) of the Supplemental Material [20]) are also shown. Extrapolations of the 50% $\rho_{\rm N}$ data in Figs. 4(b) and 4(d) give $B_{c2\perp} = 2.6$ T and $B_{c2\|} = 4.3$ T at 0 K, yielding the coherence lengths $\xi_{ab} = 11.3$ nm and $\xi_{c^*} = 6.8$ nm. The relatively small anisotropy in B_{c2} may seem strange for a superconductor with a quasi-2D Fermi surface, but a similar situation has been found in $BaFe_2As_2$-based superconductors [27,28] and is believed to be due to a finite k_z dispersion of the cylindrical Fermi surface.

The $B_{c2}(T)$ behavior expected for a conventional superconductor from the Werthamer-Helfand-Hohenberg (WHH) theory [29] tends to saturate for $T \to 0$, as shown with solid lines in Figs. 4(b) and 4(d). On the other hand, our experimental data present much weaker tendency toward saturation. We note that the Pauli paramagnetic limit [29], $B_{\rm Pauli} = 1.84T_c = 5.3$ T, is larger than our B_{c2}, so the violation of the conventional behavior is not as strong as in the case of exotic superconductors such as UBe_{13} [26]. Nevertheless, similar violations of the WHH theory to those found here

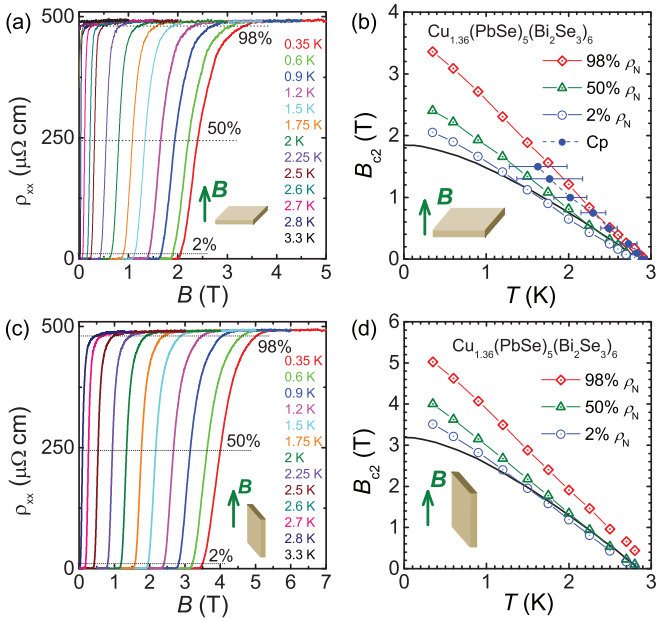

FIG. 4. (Color online) Upper critical field B_{c2}. (a) and (c) Magnetic-field-induced resistive transitions measured at various temperatures in the $x = 1.36$ sample for (a) $B \perp ab$ and (c) $B \| ab$. Three levels of the resistivity ρ_{xx} in those transitions, corresponding to 2%, 50%, and 98% of ρ_N (shown by dotted lines), are used for determining the depinning, mid-point, and onset fields, respectively; 50% ρ_N is the definition of B_{c2}. (b) and (d) B vs T phase diagrams obtained from the data in (a) and (c), respectively. The black solid lines are the conventional $B_{c2}(T)$ behavior given by the WHH theory, which is determined by the $(dB_{c2}/dT)_{T=T_c}$ value (0.936 T/K for $B \perp ab$ and 1.615 T/K for $B \| ab$). In (b), the onset temperatures of the specific-heat transitions in various magnetic fields measured in the same sample (see [20]) are also shown for comparison.

have been discussed as being indicative of unconventional superconductivity in $Cu_xBi_2Se_3$ [13] and in Bi_2Se_3 under high pressure [14].

We have further characterized the CPSBS superconductor by measuring the lower critical field B_{c1}, which was determined to be 0.34 mT for $B \| ab$ at 0 K (Fig. S6(c) of the Supplemental Material [20]). Knowing $B_{c1\|}$, $B_{c2\perp}$, and $B_{c2\|}$, one can obtain the Ginzburg-Landau parameter $\kappa_{ab} = 192$, the penetration depths $\lambda_{ab} = 1.3$ μm and $\lambda_{c^*} = 2.2$ μm, and the thermodynamic critical field $B_c = 16.6$ mT [20]. The long penetration depths are consistent with the low carrier density and moderate disorder in CPSBS.

It is striking that all the bulk properties of the superconductor CPSBS shown here point to possible occurrence of unconventional superconductivity accompanied with line nodes. The existence of line nodes implies a sign-changing gap function, which generically gives rise to surface Andreev bound states [30]. Strong spin-orbit coupling causes such surface Andreev states to be spin-split and form spin-nondegenerate Kramers pairs, which means that they become helical Majorana fermions [9]. Indeed, nodal superconductors with strong spin-orbit coupling have been discussed as being topological [11,31]. Therefore, the superconductivity in CPSBS has a good chance to be topological and harbor Majorana fermions. We should note, however, that the present data do not fully guarantee that CPSBS realizes a topological superconductivity, because a nodal gap can also be found in anisotropic s-wave superconductivity. To nail down the topological nature, making a Josephson junction with a conventional superconductor to measure a nontrivial current-phase relationship coming from boundary Majorana fermions [7,8] would be a smoking-gun experiment.

We thank T. Toba for his help in synthesizing the samples, K. Eto and M. Kriener for technical assistance, and L. Fu, Y. Tanaka, A. Taskin, and A. Yamakage for helpful discussions. This work was supported by Japan Society for the Promotion of Science (KAKENHI 24740237, 24540320, and 25220708), MEXT (Innovative Area "Topological Quantum Phenomena" KAKENHI), Air Force Office of Scientific Research (AOARD 124038), and the Inamori Foundation.

[1] X.-L. Qi and S.-C. Zhang, Rev. Mod. Phys. **83**, 1057 (2011).
[2] M. Z. Hasan and C. L. Kane, Rev. Mod. Phys. **82**, 3045 (2010).
[3] Y. Ando, J. Phys. Soc. Jpn. **82**, 102001 (2013).
[4] A. P. Schnyder, S. Ryu, A. Furusaki, and A. W. W. Ludwig, Phys. Rev. B **78**, 195125 (2008).
[5] Y. Tanaka, M. Sato, and N. Nagaosa, J. Phys. Soc. Jpn. **81**, 011013 (2012).
[6] Y. Maeno, S. Kittaka, T. Nomura, S. Yonezawa, and K. Ishida, J. Phys. Soc. Jpn. **81**, 011009 (2012).
[7] J. Alicea, Rep. Prog. Phys. **75**, 076501 (2012).
[8] C. W. J. Beenakker, Annu. Rev. Condens. Matter Phys. **4**, 113 (2013).
[9] L. Fu and E. Berg, Phys. Rev. Lett. **105**, 097001 (2010).
[10] Y. S. Hor, A. J. Williams, J. G. Checkelsky, P. Roushan, J. Seo, Q. Xu, H. W. Zandbergen, A. Yazdani, N. P. Ong, and R. J. Cava, Phys. Rev. Lett. **104**, 057001 (2010).
[11] S. Sasaki, M. Kriener, K. Segawa, K. Yada, Y. Tanaka, M. Sato, and Y. Ando, Phys. Rev. Lett. **107**, 217001 (2011).
[12] S. Sasaki, Z. Ren, A. A. Taskin, K. Segawa, L. Fu, and Y. Ando, Phys. Rev. Lett. **109**, 217004 (2012).
[13] T. V. Bay, T. Naka, Y. K. Huang, H. Luigjes, M. S. Golden, and A. de Visser, Phys. Rev. Lett. **108**, 057001 (2012).
[14] K. Kirshenbaum, P. S. Syers, A. P. Hope, N. P. Butch, J. R. Jeffries, S. T. Weir, J. J. Hamlin, M. B. Maple, Y. K. Vohra, and J. Paglione, Phys. Rev. Lett. **111**, 087001 (2013).
[15] G. Goll, M. Marz, A. Hamann, T. Tomanic, K. Grube, T. Yoshino, and T. Takabatake, Physica B **403**, 1065 (2008).
[16] N. P. Butch, P. Syers, K. Kirshenbaum, A. P. Hope, and J. Paglione, Phys. Rev. B **84**, 220504(R) (2011).
[17] K. Nakayama, K. Eto, Y. Tanaka, T. Sato, S. Souma, T. Takahashi, K. Segawa, and Y. Ando, Phys. Rev. Lett. **109**, 236804 (2012).
[18] L. Fang, C. C. Stoumpos, Y. Jia, A. Glatz, D. Y. Chung, H. Claus, U. Welp, W. K. Kwok, and M. G. Kanatzidis, Phys. Rev. B **90**, 020504(R) (2014).

[19] M. Kriener, K. Segawa, Z. Ren, S. Sasaki, and Y. Ando, Phys. Rev. Lett. **106**, 127004 (2011).
[20] See Supplemental Material at http://link.aps.org/supplemental/10.1103/PhysRevB.90.220504 for materials and methods, supplemental data, and additional discussions.
[21] T. H. Hsieh and L. Fu, Phys. Rev. Lett. **108**, 107005 (2012).
[22] M. Tinkham, *Introduction to Superconductivity* (McGraw-Hill, New York, 1975).
[23] H. Won and K. Maki, Phys. Rev. B **49**, 1397 (1994).
[24] K. Maki, in *Superconductivity*, edited by R. D. Parks (Marcel Dekker, New York, 1969).
[25] G. E. Volovik, Pis'ma v ZhETF **58**, 457 (1993) [JETP Lett. **58**, 469 (1993)].
[26] M. B. Maple, J. W. Chen, S. E. Lambert, Z. Fisk, J. L. Smith, H. R. Ott, J. S. Brooks, and M. J. Naughton, Phys. Rev. Lett. **54**, 477 (1985).
[27] H. Q. Yuan, J. Singleton, F. F. Balakirev, S. A. Baily, G. F. Chen, J. L. Luo, and N. L. Wang, Nature (London) **457**, 565 (2009).
[28] M. A. Tanatar, N. Ni, C. Martin, R. T. Gordon, H. Kim, V. G. Kogan, G. D. Samolyuk, S. L. Bud'ko, P. C. Canfield, and R. Prozorov, Phys. Rev. B **79**, 094507 (2009).
[29] N. R. Werthamer, E. Helfand, and P. C. Hohenberg, Phys. Rev **147**, 295 (1966).
[30] S. Kashiwaya and Y. Tanaka, Rep. Prog. Phys. **63**, 1641 (2000).
[31] M. Sato and S. Fujimoto, Phys. Rev. Lett. **105**, 217001 (2010).
[32] K. Momma and F. Izumi, J. Appl. Crystallogr. **44**, 1272 (2011).